AMERICAN SOCIETY of
GENE & CELL
THERAPY

Loss of lncRNA-SNHG7 Promotes the Suppression of Hepatic Stellate Cell Activation via miR-378a-3p and DVL2

Fujun Yu,[1,4] Peihong Dong,[2,4] Yefan Mao,[3] Binyu Zhao,[3] Zhiming Huang,[1] and Jianjian Zheng[3]

[1]Departments of Gastroenterology and Hepatology, The First Affiliated Hospital of Wenzhou Medical University, Wenzhou 325000, China; [2]Department of Infectious D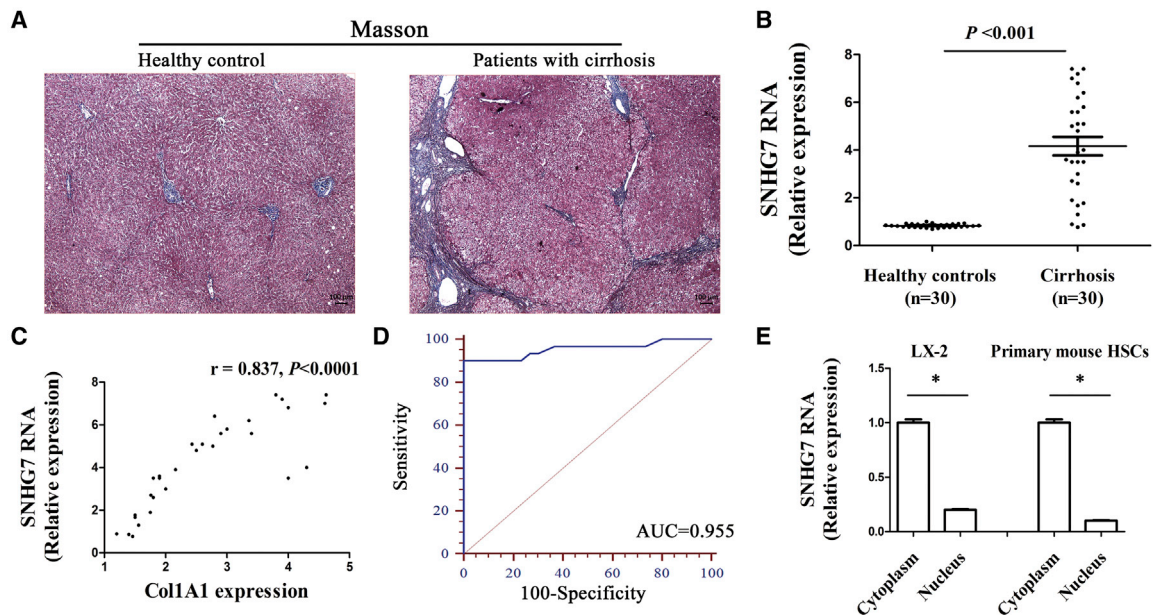iseases, The First Affiliated Hospital of Wenzhou Medical University, Wenzhou 325000, China; [3]Key Laboratory of Diagnosis and Treatment of Severe Hepato-Pancreatic Diseases of Zhejiang Province, The First Affiliated Hospital of Wenzhou Medical University, Wenzhou 325000, China

Small nuclear RNA host gene 7 (SNHG7), a novel long non-coding RNA (lncRNA), acts as an oncogene in cancers. However, whether SNHG7 is involved in hepatic stellate cell (HSC) activation during liver fibrosis is still unclear. In this study, upregulation of SNHG7 was found *in vivo* and *in vitro* during liver fibrosis. Silencing of SNHG7 led to the suppression of HSC activation, with a reduction in cell proliferation and collagen expression. SNHG7 knockdown also resulted in the suppression of liver fibrosis *in vivo*. Interestingly, miR-378a-3p was a target of SNHG7. SNHG7 and miR-378a-3p were co-located in the cytoplasm. Downregulation of miR-378a-3p blocked down the effects of loss of SNHG7 on HSC activation. Notably, SNHG7 could enhance Wnt/β-catenin pathway activation to contribute to liver fibrosis, with an increase in T cell factor (TCF) activity and a reduction in P-β-catenin level. It was found that miR-378a-mediated dishevelled segment polarity protein 2 (DVL2) was responsible for SNHG7-activated Wnt/β-catenin pathway. DVL2 was confirmed as a target of miR-378a-3p. SNHG7-induced HSC activation was almost blocked down by DVL2 knockdown. Accordingly, enhanced Wnt/β-catenin by SNHG7 was suppressed by loss of DVL2. Collectively, we demonstrate that SNHG7 reduces miR-378a-3p and attenuates its control on DVL2, leading to aberrant Wnt/β-catenin activity, which contributes to liver fibrosis progression.

INTRODUCTION

Liver fibrosis, caused by a variety of chronic and persistent liver injuries, including viral infection, alcohol consumption, and non-alcoholic fatty liver disease, is a wound-healing process.[1,2] Liver fibrosis is also a disorder between fibrogenesis and fibrinolysis, which is characterized by excessive extracellular matrix (ECM), increased collagen fiber content, and decreased ECM degradation.[3] It is well known that quiescent hepatic stellate cells (HSCs) are vitamin A storage cells. Transdifferentiation of quiescent HSCs to proliferative myofibroblasts plays a crucial role in the progression of liver fibrosis.[4] Therefore, effectively suppressing activation of HSCs is considered as a potential therapeutic target for liver fibrosis.

Long non-coding RNAs (lncRNAs), longer than 200 bp, lack of protein-coding ability.[5] Increasing evidence shows that lncRNAs are a class of key regulatory molecules in regulating chromatin dynamics, gene expression, growth, and differentiation.[6,7] lncRNAs have been reported to be involved in many critical biological processes, such as transcriptional and posttranscriptional regulation, cell cycle control, and metabolic processes.[8] Recent studies have demonstrated that dysregulations of lncRNAs are closely related to various human diseases.[9] For example, lncRNA-small nuclear RNA host gene 7 (SNHG7) contributes to the proliferation, migration, and invasion of colorectal cancer (CRC) cell lines.[10] However, the roles of SNHG7 in liver fibrosis progression are largely unknown.

RESULTS

Upregulation of SNHG7 Is Found in Human Fibrotic Liver Tissues

To explore whether SNHG7 is associated with liver fibrosis progression, SNHG7 expression was examined in human fibrotic liver tissues from patients with cirrhosis. As confirmed by Masson staining, collagen expression was significantly upregulated in patients with cirrhosis (Figure 1A). A significant increase in SNHG7 expression was found in human fibrotic liver tissues in comparison with the control (Figure 1B). There was a positive correlation between SNHG7 expression and alpha-1(I) collagen (Col1A1) mRNA level in patients with cirrhosis (r = 0.837, p < 0.0001; Figure 1C). These data suggest the possible involvement of SNHG7 in liver fibrosis. The diagnostic significance of SNHG7 in liver fibrosis was subsequently explored. As shown by receiver operating characteristic (ROC) curve analysis, liver SNHG7 had a good diagnostic value for liver fibrosis, with an

Figure 1. Expression of SNHG7 in the Liver Tissues from Patients with Cirrhosis

(A) Masson staining was performed for assessing collagen expression. Scale bar, 100 μM. (B) SNHG7 was enhanced in patients with cirrhosis (n = 30) in comparison with healthy controls (n = 30). (C) SNHG7 expression correlated with transcriptional level of Col1A1 in patients with cirrhosis. (D) ROC analysis of SNHG7 for discriminating patients with cirrhosis from healthy controls. (E) Distribution of SNHG7 expression in the cytoplasm and nucleus in human LX-2 cells as well as primary mouse HSCs. *p < 0.05.

area under the ROC curve (AUC) of 0.955 (95% confidence interval [CI], 0.868 to 0.990) (Figure 1D). In addition, it was found that its sensitivity was 90% as well as that its specificity was 100% when the cutoff value was 1.0, indicating it may be a potential diagnostic biomarker for liver fibrosis. SNHG7 was higher in the cytoplasm than that in the nucleus in human LX-2 cells (Figure 1E). The similar result was found in primary HSCs (Figure 1E).

SNHG7 Downregulation Inhibits HSC Proliferation and Collagen Expression

HSC activation is a key event in liver fibrosis, and activated HSCs have important characteristics such as high cell proliferation and accumulated collagen expression. Next, primary HSCs were isolated from healthy mice, and the detection of SNHG7 expression in primary HSCs was performed. During culture days, SNHG7 expression was gradually increased in HSCs (Figure 2A). To examine the roles of SNHG7 in HSC activation, HSCs were transduced with Ad-shSNHG7 (adenoviral vectors expressing short hairpin RNA [shRNA] against SNHG7) to silence SNHG7 expression. A significant reduction in SNHG7 expression was observed in cells after Ad-shSNHG7 treatment (Figure 2B). Loss of SNHG7 led to the suppression of HSC proliferation (Figure 2C). Generally, abnormal cell proliferation may correlate with the alteration of the cell cycle. Our results indicated that silencing of SNHG7 inhibited the cell cycle, associated with increased cells in the G0/G1 phase and reduced cells in the S phase (Figure 2D). Thus, the inhibitory effects of loss of SNHG7 on cell proliferation were through controlling transition from the G0/G1 to S phase. In addition, the effects of loss of SNHG7 on

collagen expression were examined *in vitro*. It was found that Col1A1 mRNA level was downregulated after Ad-shSNHG7 treatment (Figure 2E). Accordingly, immunofluorescence analysis indicated a reduction in type I collagen in Ad-shSNHG7 group (Figure 2F). Therefore, SNHG7 may play a pro-fibrotic role in HSC activation.

Loss of SNHG7 Attenuates Liver Fibrosis *In Vivo*

The detection of SNHG7 expression in carbon tetrachloride (CCl_4) mice indicated an enhanced SNHG7 expression in the fibrotic liver tissues (Figure 3A). Upregulation of SNHG7 expression was also found in isolated primary HSCs from CCl_4 mice at different weeks (Figure 3B). *In vivo*, Ad-shSNHG7 treatment led to the suppression of SNHG7 expression (Figure 3A). In line with it, reduced SNHG7 was found in isolated primary HSCs from CCl_4 mice after Ad-shSNHG7 treatment (Figure 3C). After silencing SNHG7, the roles of SNHG7 knockdown in CCl_4-induced liver fibrosis were investigated. As confirmed by Sirius red staining, CCl_4-caused collagen deposits were blocked down by Ad-shSNHG7 (Figures 3D and 3E). Enhanced Col1A1 mRNA by CCl_4 was significantly blocked down by loss of SNHG7 (Figure 3F). Accordingly, CCl_4-induced hydroxyproline was reduced by Ad-shSNHG7 (Figure 3G). Our results suggest that loss of SNHG7 contributes to the suppression of liver fibrosis *in vivo*.

miR-378a-3p Is a Target of SNHG7

Recent studies have shown that lncRNA could serve as competing endogenous RNAs (ceRNAs) to sponge microRNAs (miRNAs),
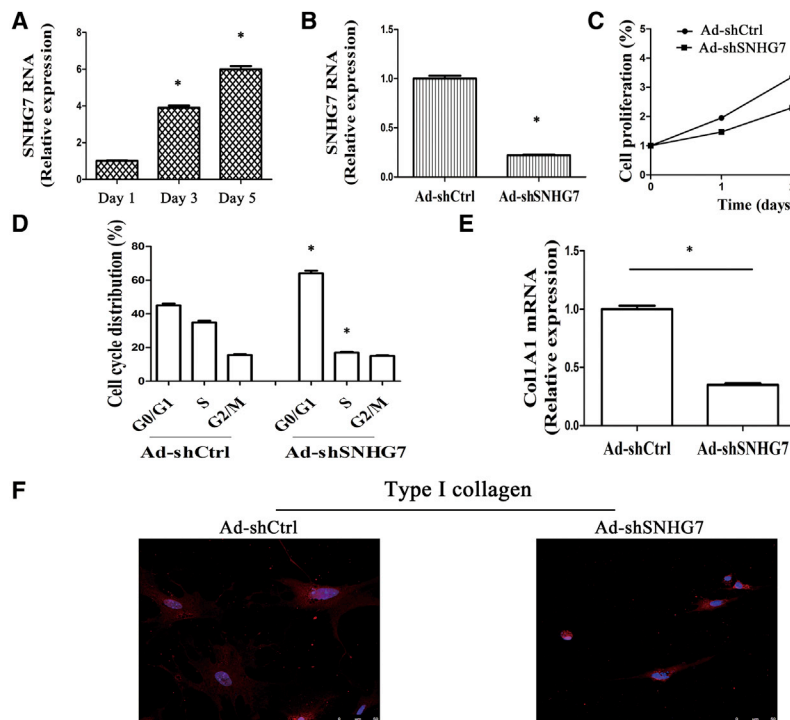
Figure 2. Effects of SNHG7 Downregulation on HSC Activation *In Vitro*

Primary 1-day-old HSCs were transduced with Ad-shSNHG7 for 48 h. (A) SNHG7 expression in primary HSCs at day 1, day 3, and day 5. Primary HSCs were isolated from healthy mice. (B) SNHG7 expression in HSCs after Ad-shSNHG7 treatment. (C) HSC proliferation in cells with Ad-shSNHG7 treatment for 24 h, 48 h, or 72 h. (D) Cell cycle. (E) Col1A1 mRNA expression level. (F) Immunofluorescence staining for type I collagen (red) was analyzed by confocal laser microscopy in cells after Ad-shSNHG7 treatment. DAPI-stained nuclei, blue. *p < 0.05 compared with the control.

leading to the derepression of miRNA targets.[11] Due to the main expression of SNHG7 in the cytoplasm, we hypothesized that SNHG7 may act as a ceRNA for miRNAs to regulate the activity of miRNAs. To determine it, an RNA binding protein immunoprecipitation (RIP) experiment with an antibody against Argonaute-2 (Ago2) was performed. The results of RIP revealed that SNHG7 was enriched by 8.6-fold in the Ago2 pellet compared with that in immunoglobulin G (IgG) pellets (Figure 4A), indicating that SNHG7 could act as a binding platform for Ago2 and miRNAs. Bioinformatic analysis (miRanda and RNAhybrid) was used to analyze the potential miRNAs that may bind to SNHG7. miRNAs, including miR-135a-1-3p, miR-149-5p, miR-378a-3p, miR-351-3p, miR-139-3p, miR-540-3p, miR-667-5p, miR-672-5p, miR-504-3p, and miR-129b-3p, were predicted to bind to SNHG7. Luciferase activity assays were performed to examine whether these miRNA recognition sequences on SNHG7 could be affected by the predicted miRNAs. It was found that all predicted miRNAs reduced the luciferase reporter activities (Figure 4B). However, only miR-378a-3p could reduce the luciferase reporter activity by at least 70%. Therefore, miR-378a-3p was chosen for the next experiment. The target sites for miR-378a-3p from the luciferase reporter were mutated (Figure 4C). It was found that miR-378a-3p resulted in a reduction in luciferase activity of SNHG7-Wt, while it had no effect on SNHG7-Mut luciferase activity (Figure 4C). Pull-down assay was performed to further confirm this interaction. As expected, SNHG7 enrichment was enhanced in the biotinylated miR-378a-3p (Bio-miR-378a-3p) group (Figure 4D). However, no significant change was found in the Bio-miR-378a-3p-Mut group. Notably, the results of fluorescence *in situ* hybridization (FISH) indicated a co-localization between

miR-378a-3p and SNHG7 in the cytoplasm (Figure 4E). Combined with these, miR-378a-3p is a target of SNHG7.

Loss of SNHG7 Contributes to the Suppression of HSC Activation via miR-378a-3p

Whether miR-378a-3p was involved in the effects of SNHG7 on HSC activation was examined. We first examined miR-378a-3p levels in fibrotic liver tissues as well as activated HSCs. miR-378a-3p was shown to be downregulated in patients with cirrhosis (Figure 5A). Reduced miR-378a-3p was found in primary HSCs during HSC activation (Figure 5B). Moreover, miR-378a-3p was downregulated in a time-dependent manner in isolated primary HSCs from CCl₄ mice at different weeks (Figure 5C). There was a negative correlation between SNHG7 and miR-378a-3p. SNHG7 was downregulated by miR-378a-3p mimics and upregulated by the miR-378a-3p inhibitor (Figure 5D). Overexpression of SNHG7 reduced miR-378a-3p, while loss of SNHG7 enhanced miR-378a-3p (Figure 5E). Of note, SNHG7 knockdown-induced the suppression of HSC proliferation was reversed by the miR-378a-3p inhibitor (Figure 5F). Downregulation of Col1A1 mRNA caused by loss of SNHG7 was inhibited by the miR-378a-3p inhibitor (Figure 5G). In line with the mRNA result, reduced type I collagen by SNHG7 downregulation was rescued by the miR-378a-3p inhibitor (Figure 5H). To sum up, these results demonstrate that loss of SNHG7 contributes to the suppression of HSC activation, at least in part, through sponging miR-378a-3p.

SNHG7 Accelerates HSC Activation through miR-378a-Mediated Dishevelled Segment Polarity Protein 2 (DVL2)

Aberrant Wnt/β-catenin pathway has been reported to participate in the progression of liver fibrosis. Herein, overexpression of SNHG7 caused an increase in T cell factor (TCF) activity as well as a reduction in P-β-catenin and glycogen synthase kinase-3β (GSK-3β), indicating that Wnt/β-catenin pathway activity was enhanced by SNHG7 (Figures 6A and 6B). Due to the fact that SNHG7 plays a role in liver fibrosis by sponging miR-378a-3p, it was necessary to identify the potential targets of miR-378a-3p. Using bioinformatic
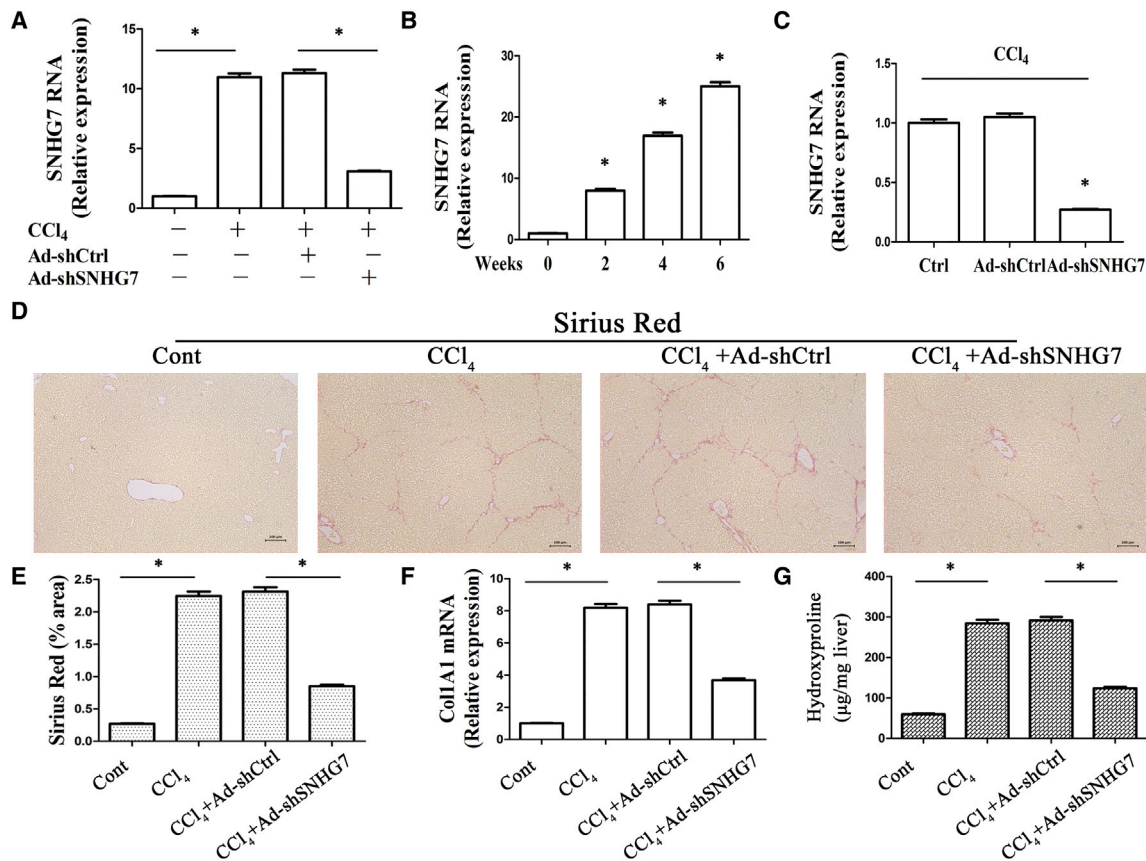
Figure 3. Effects of Loss of SNHG7 on CCl₄-Induced Liver Fibrosis *In Vivo*

(A) SNHG7 expression in CCl$_4$ mice after Ad-shSNHG7 treatment. (B) SNHG7 expression in primary HSCs isolated from CCl$_4$ mice at different weeks. (C) SNHG7 expression in primary HSCs isolated from CCl$_4$ mice after Ad-shSNHG7 treatment. (D) Collagen expression was assessed by Sirius red staining. Scale bars, 100 μm. (E) The Masson stain-positive areas were analyzed in the liver tissues. (F) Col1A1 mRNA level. (G) Hydroxyproline level. *$p < 0.05$ compared with the control.

analysis (http://www.microrna.org/microrna/getMirnaForm.do), DVL2, a component of the Wnt/β-catenin pathway, was predicted as a putative target of miR-378a-3p (Figure 6C). As shown in Figure 6D, luciferase reporter assays confirmed that DVL2 was a target of miR-378a-3p. The mRNA and protein expression level of DVL2 were increased during culture days (Figure 6E). Interestingly, loss of DVL2 blocked down the effects of SNHG7 on HSC activation, with a reduction in cell proliferation, α-smooth muscle actin (α-SMA), and Col1A1 (Figures 6F and 6G). Moreover, enhanced Wnt/β-catenin pathway activity by SNHG7 was inhibited by silencing of DVL2 (Figures 6A and 6B). Our results suggest that SNHG7 activates Wnt/β-catenin pathway to accelerate HSC activation through miR-378a-mediated DVL2.

DISCUSSION

SNHG7, a potential oncogene, has been reported to be upregulated in many cancer tissues and cell lines.[12–14] Loss of SNHG7 contributes to the suppression of cell proliferation and the induction of cell apoptosis through miR-193b in non-small-cell lung cancer.[15] The results of the present study showed that silencing of SNHG7 inhibited

liver fibrosis progression *in vivo* and *in vitro*. Owing to downregulation of miR-378a-3p caused by SNHG7, DVL2 expression was enhanced, resulting in the activation of Wnt/β-catenin and liver fibrosis progression. Further studies showed that SNHG7 and DVL2 were targets of miR-378a-3p. These data indicate that loss of SNHG7 contributes to the suppression of liver fibrosis, at least in part, through miR-378a-3p and DVL2.

Numerous studies have shown that lncRNAs, deregulated in various human diseases including cancers, could participate in a wide range of biological processes through diverse molecular mechanisms including chromatin modification, transcriptional regulation, and post-transcriptional regulation.[6,16] Among post-transcriptional regulation, lncRNA could serve as ceRNA to sponge miRNAs, leading to the derepression of miRNA targets. For example, we previously found that homeobox transcript antisense RNA (HOTAIR) suppresses phosphatase and tensin homolog (PTEN) expression via sponging miR-29b.[17] SNHG7 has been reported to sponge miR-216b to accelerate proliferation and liver metastasis of CRC, suggesting that SNHG7 could bind to miRNAs.[10] In this study, we found that
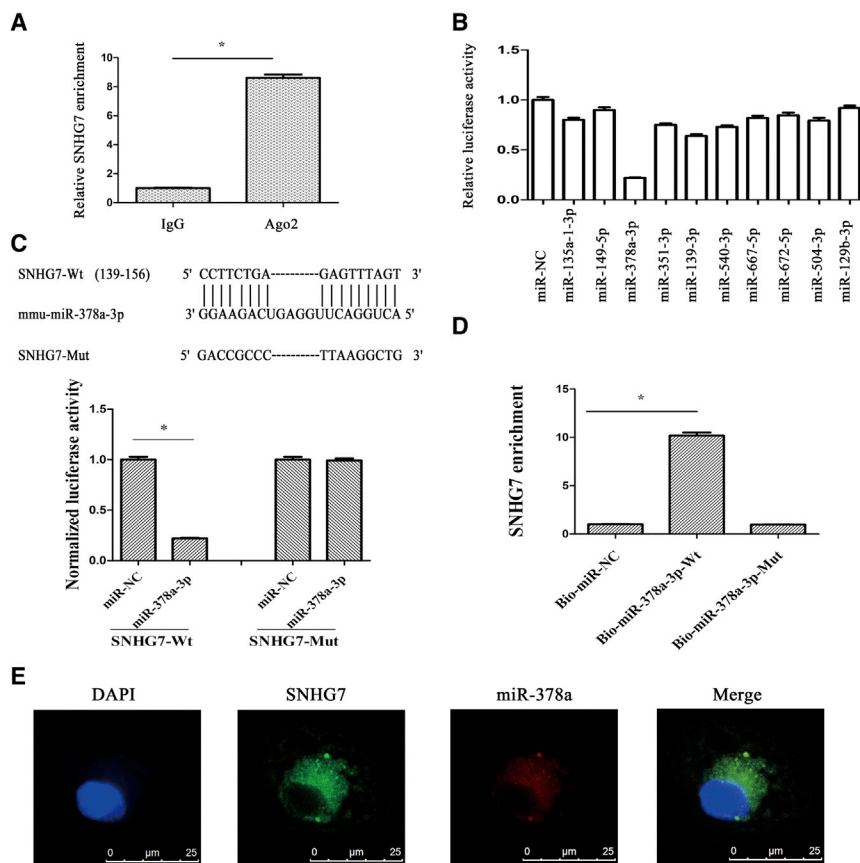
Figure 4. miR-378a-3p Is a Target of SNHG7

(A) RIP experiments were performed using Ago2 antibody on extracts from primary HSCs. Relative expression level of SNHG7 was expressed as fold enrichment in Ago2 relative to IgG immunoprecipitates by qRT-PCR. (B) The luciferase activity of pmirGLO-SNHG7-Wt in HEK293T cells after co-transfection with the indicated 10 miRNAs or miR-NC. (C) A schematic drawing indicated the putative binding sites of miR-378a-3p with respect to SNHG7. Relative luciferase activities of pmirGLO-SNHG7-Wt or pmirGLO-SNHG7-Mut were analyzed in HEK293T cells after co-transfection with miR-378a-3p or miR-NC. (D) Interaction between SNHG7 and miR-378a-3p was confirmed by pull-down assay. Bio-miR-NC is not complementary to SNHG7. (E) Co-localization between miR-378a-3p and SNHG7 was observed by RNA in situ hybridization. *$p < 0.05$.

silencing of DVL2 resulted in the suppression of SNHG7-induced Wnt/β-catenin activation, with a reduction in TCF activity as well as an increase in P-β-catenin and GSK-3β. To sum up, SNHG7 enhances Wnt/β-catenin activity to contribute to HSC activation via miR-378-3p and DVL2 (Figure 6H). Moreover, miR-378a-3p has a feedback regulation to SNHG7 expression (Figure 6H).

Recently, emerging data have shown that lncRNAs could serve as promising biomarkers for diagnosis and/or prognosis of many human diseases. For example, Xia et al. reported that metastasis-associated lung adenocarcinoma transcript 1 (MALAT1) could function as an oncogene in gastric cancer, and high MALAT1 levels could serve as a potential biomarker for the distant metastasis of gastric cancer.[21] Herein, SNHG7 was upregulated in patients with cirrhosis compared with healthy controls. ROC curve analysis indicated that liver SNHG7 had a good diagnostic value for liver fibrosis, with a high sensitivity and specificity. These data suggest that liver SNHG7 may be a potential biomarker in liver fibrosis. However, studies with a larger sample size are warranted to validate the clinical significance of this biomarker.

In conclusion, we demonstrate that loss of SNHG7 contributes to the suppression of HSC activation, at least in part, through miR-378a-3p and DVL2. We disclose a novel SNHG7/miR-378a-3p/ DVL2 signaling cascade in liver fibrosis.

SNHG7 was mainly expressed in the cytoplasm. A RIP experiment showed that SNHG7 could be recruited to Ago2-related RNA-induced silencing complexes to serve as a miRNA-binding platform. Using bioinformatic analysis and luciferase reporter assays, miR-378a-3p was confirmed as a target of SNHG7. Pull-down assay confirmed the interaction between SNHG7 and miR-378a-3p. Next, the co-localization between miR-378a-3p and SNHG7 was found in the cytoplasm. Further studies showed that the inhibitory effects of loss of SNHG7 on HSC activation were inhibited by miR-378a-3p inhibitor. Taken together, our data suggest that loss of SNHG7 inhibits HSC activation, at least in part, through sponging miR-378a-3p.

Aberrant Wnt/β-catenin pathway has been reported to play a crucial role in liver fibrosis.[18] Activated Wnt/β-catenin promotes HSC activation, whereas antagonizing Wnt/β-catenin attenuates HSC activities.[19,20] The results of the present study showed that SNHG7 induced Wnt/β-catenin activation, with an increase in TCF activity as well as a reduction in phosphorylated (P)-β-catenin and GSK-3β. Due to the binding between SNHG7 and miR-378a-3p, the potential Wnt/β-catenin-related targets of miR-378a-3p were predicted and examined. Interestingly, DVL2, a member of the Wnt/β-catenin pathway, was confirmed to be a target of miR-378a-3p. DVL2 was increased during liver fibrosis, and downregulated DVL2 led to the suppression of SNHG7-mediated HSC activation. In addition,

MATERIALS AND METHODS

Materials

miR-378a-3p mimics, miR-378a-3p inhibitor, and negative control (miR-NC) were purchased from GenePharma biotechnology (Shanghai, China). For transfection, cells were transfected with 1 μg of chemically synthesized miRNA. Ad-shSNHG7, adenoviral vectors
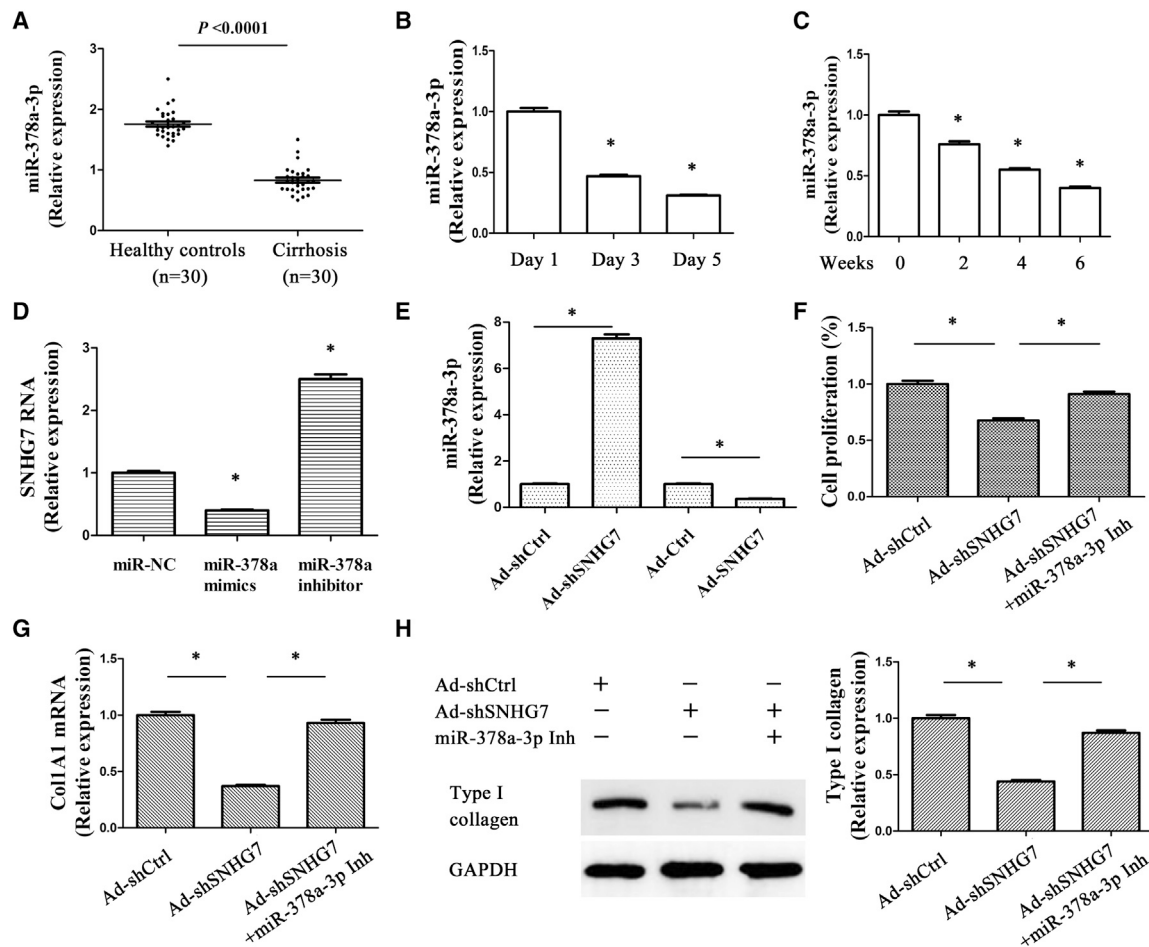
Figure 5. Anti-fibrotic Effects of Loss of SNHG7 through miR-378a-3p

Primary 1-day-old HSCs were transduced with Ad-shSNHG7 for 48 h and treated with miR-378a-3p inhibitor for additional 48 h. (A) miR-378a-3p expression in patients with cirrhosis. (B) miR-378a-3p expression in primary HSCs at day 1, day 3, and day 5. Primary HSCs were isolated from healthy controls. (C) miR-378a-3p expression in primary HSCs isolated from CCl_4 mice at different weeks. (D) SNHG7 expression. (E) miR-378a-3p level. (F) Reduced cell proliferation by loss of SNHG7 was restored by miR-378a-3p inhibitor. (G) SNHG7 knockdown induced the reduction in Col1A1 mRNA was reversed by miR-378a-3p inhibitor. (H) Reduced type I collagen expression by loss of SNHG7 was blocked down by miR-378a-3p inhibitor. *p < 0.05 compared to the control.

expressing scrambled shRNA (Ad-shCtrl), adenoviral vectors expressing SNHG7 (Ad-SNHG7), and adenoviral vectors expressing a control scrambled sequence (Ad-Ctrl) were obtained from Gene-Pharma biotechnology.

Clinical Human Specimens

Written informed consent was received from all patients prior to obtaining liver tissues. In this study, 30 healthy controls and 30 liver-cirrhosis patients undergoing partial liver resection or liver biopsy were selected from the First Affiliated Hospital of Wenzhou Medical University. Liver cirrhosis was diagnosed by liver biopsy and/or a typical appearance of the liver on abdominal ultrasound and/or computed tomography scan. This study was performed in compliance with the Declaration of Helsinki and approved by the Ethics Committee of the First Affiliated Hospital of Wenzhou Medical University.

CCl_4 Liver Injury Model

Eight-week-old male C57BL/6J mice (n = 6) received intraperitoneal injection of 7 μL/g of 10% CCl_4 (Sigma-Aldrich, St. Louis, MO, USA) in olive oil two times weekly for 6 weeks. Also, mice (n = 6) treated with olive oil treatment were considered as the control mice. As well as oil treatment and CCl_4 treatment, mice additionally received CCl_4 in combination with Ad-shCtrl (n = 6) and CCl_4 in combination with Ad-shSNHG7 (n = 6). Ad-shSNHG7 (1×10^9 PFU/100 μL) was injected every 2 weeks by way of the tail vein for 6 weeks. All animals were provided by the Experimental Animal Center of Wenzhou Medical University. The animal experimental protocol was approved by the University Animal Care and Use Committee. Mice were sacrificed under anesthesia after CCl_4 treatment. The livers from mice were removed for further analysis. The liver tissues were used for Sirius red staining.
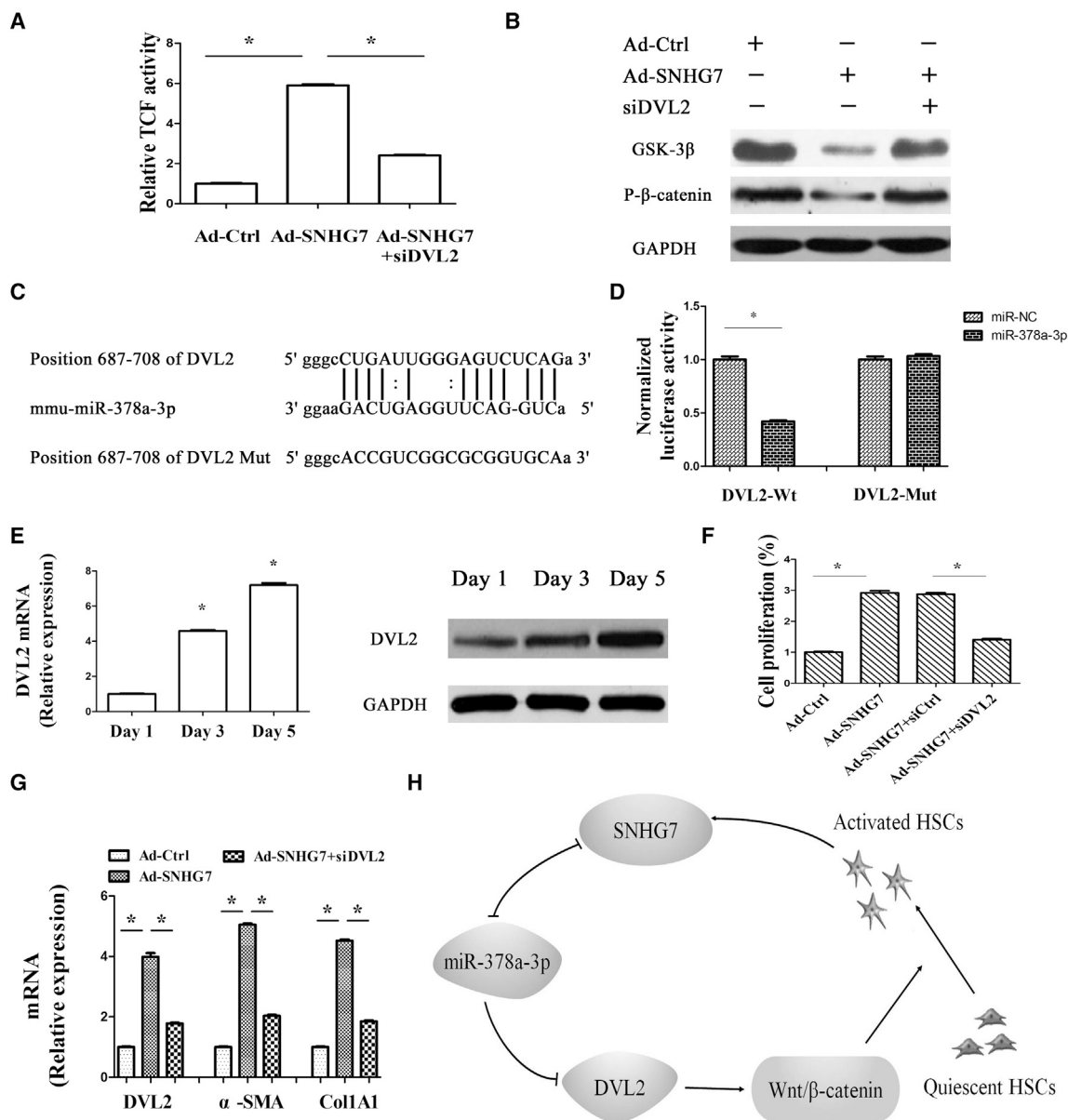
Figure 6. Loss of SNHG7 Inhibited Wnt/β-Catenin and HSC Activation via DVL2

Primary 1-day-old HSCs were transduced with Ad-SNHG7 for 48 h and transfected with DVL2 siRNA for an additional 48 h. (A) TCF activity. (B) Levels of P-β-catenin and GSK-3β. (C) A schematic drawing indicated the putative binding sites of miR-378a-3p with respect to DVL2. (D) Relative luciferase activities of pmirGLO-DVL2-Wt or pmirGLO-DVL2-Mut were analyzed in HEK293T cells after co-transfection with miR-378a-3p or miR-NC. (E) DVL2 expression. (F) Cell proliferation. (G) The mRNA expressions of DVL2, α-SMA, and Col1A1. (H) The signal pathway was discovered in liver fibrosis.

Hepatic Hydroxyproline Content

Liver tissues (50 mg) were homogenized in HCl and hydrolyzed at 120°C overnight. After lysate centrifugation at $12,000 \times g$ for 10 min at 4°C, the supernatant was evaporated to dryness under vacuum. The hepatic hydroxyproline content was assessed using a hydroxyproline colorimetric assay kit (BioVision, San Francisco, CA, USA). Data were normalized to liver weight.

Isolation and Culture of Primary HSCs

Primary HSCs were isolated as described previously.[22] The isolated cells were seeded in tissue culture plates and cultured in DMEM with 10% fetal bovine serum, 100 U/mL penicillin, and 100 μg/mL streptomycin. The purity of cultures was confirmed by immunocytochemical staining for α-SMA and the purity reached > 98%.

LX-2 Cell Culture

The human LX-2 cell strain was obtained from JENNIO Biological Technology, Guangdong, China. It was cultured in DMEM containing 10% fetal bovine serum, 100 U/mL penicillin G sodium salt, and 100 U/mL streptomycin sulfate (Gibco, Carlsbad, CA, USA). The cells were grown in a 37°C incubator with 5% CO_2.

qRT-PCR

Total RNA was extracted from cells and liver tissues using a miRNeasy mini kit (QIAGEN, Valencia, CA, USA). Fifty nanograms RNA was reverse-transcribed to cDNA using the ReverTra Ace qPCR RT kit (Toyobo, Osaka, Japan) in accordance with the manufacturer's instructions. Cytoplasmic or nuclear SNHG7 was isolated from HSCs using cytoplasmic and nuclear RNA purification kits (Norgen, Thorold, Canada) as detailed previously.[23] Gene expression was measured by real-time PCR using cDNA, SYBR green real-time PCR master mix (Toyobo, Osaka, Japan), and a set of gene-specific oligonucleotide primers (human SNHG7, forward 5′-GCCCTGC AGCCTCGC-3′, reverse 5′-CAGCGGCGCCTCCTC-3′; mouse SNHG7, forward 5′-CC ATCCATACAGGCCTTGGG-3′, reverse 5′-AGGGTCCTCCATCC AGTGTT-3′; mouse DVL2, forward 5′-AGTCAGCTCT CATGTT GAGGGT-3′, reverse 5′-TACCCAGCCCACACCTTCTT-3′). The primers of Col1A1 and glyceraldehyde-3-phosphate dehydrogenase (GAPDH) were designed as described previously.[17,24] TaqMan microRNA assays (Applied Biosystems, Foster City, CA, USA) were performed to detect miRNA expression. The GAPDH (Applied Biosystems, Foster City, CA, USA) level was used to normalize the relative abundance of SNHG7 and mRNAs. U6 small nuclear RNA (snRNA) (Applied Biosystems, Foster City, CA, USA) was used to normalize the relative abundance of miRNAs. The expression levels ($2^{-\Delta\Delta CT}$) of SNHG7, mRNAs, and miRNAs were calculated.[25]

Western Blot Analysis

Cells were lysed with ice-cold lysis buffer (50 mM Tris-HCl [pH 7.4], 100 mM 2-mercaptoethanol, 2% [w/v] SDS, 10% glycerol). Proteins were subjected to SDS-PAGE and transferred to polyvinylidene fluoride (PVDF) membranes (Millipore, Billerica, MA, USA). After blocking, membranes were incubated with primary antibodies against type I collagen, DVL2, phosphorylated β-catenin (Y86), glycogen synthase kinase-3β (GSK-3β) and GAPDH (Abcam, Cambridge, MA, USA) overnight at 4°C, followed by secondary goat anti-rabbit IgG (Rockland, Limerick, PA, USA) at 37°C for 1 h. GAPDH served as an internal control.

Cell Proliferation Analysis

Cells were seeded in 96-well plates at a density of 1×10^3 cells per well and cultured for 24 h. Next, cells were transduced with Ad-shSNHG7 for 24 h, 48 h, or 72 h. Then, cell proliferation was evaluated using cell counting kit-8 (CCK-8; Dojindo, Kumamoto, Japan) according to manufacturer's instructions. Absorbance was determined at 450 nm on a microplate reader (Molecular Devices, Sunnyvale, CA, USA).

Immunofluorescence Microscopy

Cells were seeded on 18-mm cover glasses and fixed in an acetic acid:-ethanol (1:3) solution for 5 min at −20°C. 5% goat serum/PBS was used to block non-specific binding for 1 h at room temperature. Next, cells were incubated with primary antibodies against type I collagen at 4°C overnight, followed by fluorescein-labeled secondary antibody at 37°C for 1 h (1:50 dilution; Dianova). The nuclei were stained with DAPI. The slides were washed twice with PBS, covered with DABCO (Sigma-Aldrich), and examined with confocal laser scanning microscopy (Olympus, Tokyo, Japan) at 568 nm.

RIP Assay

The RIP experiment was conducted using the EZ-Magna RIP kit (Millipore) according to the manufacturer's instructions. In brief, primary HSCs at 80%–90% confluency were lysed in complete RIP lysis buffer, followed by incubation with RIP buffer including magnetic beads coupled with anti-Ago2 antibody (Abcam). Isotype-matched IgG was used as a negative control. After samples were incubated with Proteinase K, immunoprecipitated RNA was isolated. qRT-PCR was performed to analyze SNHG7 level in the precipitates.

Pull-Down Assay with Bio-miR-378a-3p

Biotin pull-down was performed as previously described.[26,27] In brief, after 48 h of HSCs transfected with Bio-miR-378a-3p-Wt, Bio-miR-378a-3p-Mut, or Bio-miR-NC, the cells were washed with PBS followed by incubation in a lysis buffer for 10 min. To exclude RNA and protein complexes, the beads were blocked in lysis buffer including RNase-free BSA and yeast tRNA (Sigma). After the lysates were incubated with streptavidin-coated magnetic beads (Life Technologies) at 4°C for 4 h, they were washed twice with lysis buffer, three times with low-salt buffer, and once with high-salt buffer. The bound RNAs were isolated using TRIzol reagent (Life Technologies). SNHG7 expression was determined by qRT-PCR.

Luciferase Reporter Assay

pmirGLO-SNHG7 was cotransfected with the predicted miRNAs or miR-NC into HEK293T cells by lipofectamine-mediated gene transfer as described previously.[17] The relative luciferase activity was normalized to Renilla luciferase activity 48 h after transfection.

TCF Reporter Activity Assay

Cells were transiently transfected with TOPFLASH and FOPFLASH (Upstate Biotechnology, Lake Placid, NY, USA) using Lipofectamine 2000. Twenty-four hours after transfection, the cells were harvested and luciferase and Renilla luminescence were measured using the dual-luciferase reporter assay system (Promega, Fitchburg, WI, USA) on a luminometer (BioTek Instruments, Winooski, VT, USA). TCF reporter activity was presented as the ratio of firefly-to-Renilla luciferase activity.

FISH

The double FISH assay was performed in cells as previously described,[28] with minor modifications. Biotin-labeled probes

specific to SNHG7 and Dig-labeled miR-378a-3p probes were used in the hybridization. The signals of biotin-labeled probes were detected using Cy5-Streptavidin (Life Technologies). The signals of Dig-labeled miR-378a-3p probes were detected using a tyramide-conjugated Alexa 488 fluorochrome TSA kit. Nuclei were counterstained with DAPI. Images were acquired on a Leica TCS SP2 AOBS confocal microscope (Leica Microsystems, Mannheim, Germany).

Statistical Analysis

Data from at least three independent experiments were expressed as the mean ± SD. Differences between multiple groups were evaluated using one-way ANOVA. Differences between the two groups were compared using a Student's t test. The Mann-Whitney test was performed to determine clinical significance of liver SNHG7. Pearson's test was used for the correlation analysis between the two groups. ROC curve was generated to evaluate the diagnostic potential of SNHG7 via calculation of the AUC, sensitivity, and specificity according to the standard formulas. $p < 0.05$ was considered significant. All statistical analyses were performed with SPSS software (version 13; SPSS, Chicago, IL, USA).

AUTHOR CONTRIBUTIONS

F.Y. and J.Z. carried out most of the experiments; F.Y. and Z.H. provided the statistical support; P.D. and J.Z. designed the study and analyzed the data; Y.M. and B.Z. contributed to some of the experiments. All the authors contributed to the manuscript preparation and gave final approval of the submitted manuscript.

CONFLICTS OF INTEREST

The authors declare no competing interests.

ACKNOWLEDGMENTS

REFERENCES

1. Friedman, S.L. (2008). Mechanisms of hepatic fibrogenesis. Gastroenterology 134, 1655–1669.

2. Gressner, O.A., Rizk, M.S., Kovalenko, E., Weiskirchen, R., and Gressner, A.M. (2008). Changing the pathogenetic roadmap of liver fibrosis? Where did it start; where will it go? J. Gastroenterol. Hepatol. 23, 1024–1035.

3. Yu, F., Fan, X., Chen, B., Dong, P., and Zheng, J. (2016). Activation of Hepatic Stellate Cells is Inhibited by microRNA-378a-3p via Wnt10a. Cell. Physiol. Biochem. 39, 2409–2420.

4. Roeb, E. (2018). Matrix metalloproteinases and liver fibrosis (translational aspects). Matrix Biol. 68–69, 463–473.

5. Khalil, A.M., Guttman, M., Huarte, M., Garber, M., Raj, A., Rivea Morales, D., Thomas, K., Presser, A., Bernstein, B.E., van Oudenaarden, A., et al. (2009). Many human large intergenic noncoding RNAs associate with chromatin-modifying complexes and affect gene expression. Proc. Natl. Acad. Sci. USA 106, 11667–11672.

6. Shi, X., Sun, M., Liu, H., Yao, Y., and Song, Y. (2013). Long non-coding RNAs: a new frontier in the study of human diseases. Cancer Lett. 339, 159–166.

7. Xiang, J.F., Yin, Q.F., Chen, T., Zhang, Y., Zhang, X.O., Wu, Z., Zhang, S., Wang, H.B., Ge, J., Lu, X., et al. (2014). Human colorectal cancer-specific CCAT1-L lncRNA regulates long-range chromatin interactions at the MYC locus. Cell Res. 24, 513–531.

8. Yu, F., Jiang, Z., Chen, B., Dong, P., and Zheng, J. (2017). NEAT1 accelerates the progression of liver fibrosis via regulation of microRNA-122 and Kruppel-like factor 6. J. Mol. Med. (Berl.) 95, 1191–1202.

9. Taft, R.J., Pang, K.C., Mercer, T.R., Dinger, M., and Mattick, J.S. (2010). Non-coding RNAs: regulators of disease. J. Pathol. 220, 126–139.

10. Shan, Y., Ma, J., Pan, Y., Hu, J., Liu, B., and Jia, L. (2018). LncRNA SNHG7 sponges miR-216b to promote proliferation and liver metastasis of colorectal cancer through upregulating GALNT1. Cell Death Dis. 9, 722.

11. Gu, J., Wang, Y., Wang, X., Zhou, D., Zhou, M., and He, Z. (2018). Effect of the LncRNA GAS5-MiR-23a-ATG3 Axis in Regulating Autophagy in Patients with Breast Cancer. Cell. Physiol. Biochem. 48, 194–207.

12. Deng, Y., Zhao, F., Zhang, Z., Sun, F., and Wang, M. (2018). Long Noncoding RNA SNHG7 Promotes the Tumor Growth and Epithelial-to-Mesenchymal Transition via Regulation of miR-34a Signals in Osteosarcoma. Cancer Biother. Radiopharm. Published online November 2, 2018. https://doi.org/10.1089/cbr.2018.2503.

13. Qi, H., Wen, B., Wu, Q., Cheng, W., Lou, J., Wei, J., Huang, J., Yao, X., and Weng, G. (2018). Long noncoding RNA SNHG7 accelerates prostate cancer proliferation and cycle progression through cyclin D1 by sponging miR-503. Biome. Pharmacother. 102, 326–332.

14. Ren, J., Yang, Y., Xue, J., Xi, Z., Hu, L., Pan, S.J., and Sun, Q. (2018). Long noncoding RNA SNHG7 promotes the progression and growth of glioblastoma via inhibition of miR-5095. Biochem. Biophys. Res. Commun. 496, 712–718.

15. She, K., Yan, H., Huang, J., Zhou, H., and He, J. (2018). miR-193b availability is antagonized by lncRNA-SNHG7 for FAIM2-induced tumour progression in non-small cell lung cancer. Cell Prolif. 51, https://doi.org/10.1111/cpr.12406.

16. Xing, C.Y., Hu, X.Q., Xie, F.Y., Yu, Z.J., Li, H.Y., Bin-Zhou, Wu, J.B., Tang, L.Y., and Gao, S.M. (2015). Long non-coding RNA HOTAIR modulates c-KIT expression through sponging miR-193a in acute myeloid leukemia. FEBS Lett. 589, 1981–1987.

17. Yu, F., Chen, B., Dong, P., and Zheng, J. (2017). HOTAIR Epigenetically Modulates PTEN Expression via MicroRNA-29b: A Novel Mechanism in Regulation of Liver Fibrosis. Mol. Ther. 25, 205–217.

18. Yu, F., Lu, Z., Huang, K., Wang, X., Xu, Z., Chen, B., Dong, P., and Zheng, J. (2016). MicroRNA-17-5p-activated Wnt/β-catenin pathway contributes to the progression of liver fibrosis. Oncotarget 7, 81–93.

19. Kordes, C., Sawitza, I., and Häussinger, D. (2008). Canonical Wnt signaling maintains the quiescent stage of hepatic stellate cells. Biochem. Biophys. Res. Commun. 367, 116–123.

20. Guo, Y., Xiao, L., Sun, L., and Liu, F. (2012). Wnt/beta-catenin signaling: a promising new target for fibrosis diseases. Physiol. Res. 61, 337–346.

21. Xia, H., Chen, Q., Chen, Y., Ge, X., Leng, W., Tang, Q., Ren, M., Chen, L., Yuan, D., Zhang, Y., et al. (2016). The lncRNA MALAT1 is a novel biomarker for gastric cancer metastasis. Oncotarget 7, 56209–56218.

22. Chang, W., Yang, M., Song, L., Shen, K., Wang, H., Gao, X., Li, M., Niu, W., and Qin, X. (2014). Isolation and culture of hepatic stellate cells from mouse liver. Acta Biochim. Biophys. Sin. (Shanghai) 46, 291–298.

23. Zaghlool, A., Ameur, A., Nyberg, L., Halvardson, J., Grabherr, M., Cavelier, L., and Feuk, L. (2013). Efficient cellular fractionation improves RNA sequencing analysis of mature and nascent transcripts from human tissues. BMC Biotechnol. 13, 99.

24. Han, D., Li, J., Wang, H., Su, X., Hou, J., Gu, Y., Qian, C., Lin, Y., Liu, X., Huang, M., et al. (2017). Circular RNA circMTO1 acts as the sponge of microRNA-9 to suppress hepatocellular carcinoma progression. Hepatology 66, 1151–1164.

25. Schmittgen, T.D., and Livak, K.J. (2008). Analyzing real-time PCR data by the comparative C(T) method. Nat. Protoc. *3*, 1101–1108.

26. Yu, F., Zheng, J., Mao, Y., Dong, P., Lu, Z., Li, G., Guo, C., Liu, Z., and Fan, X. (2015). Long Non-coding RNA Growth Arrest-specific Transcript 5 (GAS5) Inhibits Liver Fibrogenesis through a Mechanism of Competing Endogenous RNA. J. Biol. Chem. *290*, 28286–28298.

27. Wang, K., Liu, F., Zhou, L.Y., Long, B., Yuan, S.M., Wang, Y., Liu, C.Y., Sun, T., Zhang, X.J., and Li, P.F. (2014). The long noncoding RNA CHRF regulates cardiac hypertrophy by targeting miR-489. Circ. Res. *114*, 1377–1388.

28. Yu, J., Xu, Q.G., Wang, Z.G., Yang, Y., Zhang, L., Ma, J.Z., Sun, S.H., Yang, F., and Zhou, W.P. (2018). Circular RNA cSMARCA5 inhibits growth and metastasis in hepatocellular carcinoma. J. Hepatol. *68*, 1214–1227.